Dual Stage Four Grid (DS4G) Ion Engine for Very High Velocity Change Missions

IEPC 2009-157

31st International Electric Propulsion Conference, Ann Arbor, Michigan, USA
September 20-24, 2009

R. Intini Marques[1], S.B. Gabriel[2]
University of Southampton, Astronautics Research Group, Southampton, SO17 1BJ, United Kingdom.

ABSTRACT

Electric Propulsion (EP) was first envisioned as a revolutionary method of producing thrust and was initially aimed at main propulsion applications. Due to the frustration of the high power requirements, electric propulsion devices were soon abandoned for this application. Later, EP devices with different principles of operation were envisioned, built and investigated and many of them have increasingly found practical applications in spacecrafts. Today many EP devices are employed in space for various types of missions. Despite of still not being practical to be used as a main propulsion system for launching from the Earth, EP devices have been used as main propulsion systems for spacecrafts departing from the Earth's orbit. In the future there will be a high demand for propulsion devices able to propel spacecrafts for tasks such as Earth-Moon cargo, Earth-Mars Cargo, outer Solar System exploration and interstellar missions. These missions, requiring ΔV in the $36\ km/s$ to $72\ km/s$ range and specific impulses in the $15000 s$ to $30000 s$, find EP devices an enabling technology. This paper analyzes the theoretical performance of a high power dual stage four grid ion engine (DS4G), in the 25kW-30kW range, for use in selected very high total velocity change missions. An initial comparison with the regular 2 and 3-grid gridded ion engine is also presented with its limitations and the respective motivations for the use of the DS4G design.

1. Introduction and Background

Existing gridded ion engines (GIE) of two and three grids (GIE2 and GIE3, respectively) are able to provide specific impulses in the 2000-10000s range [1] with an experimental GIE able to achieve 19300s [2]. However, the GIE2 and GIE3 have an intrinsic compromise between maximum current density and specific impulse, which limits the maximum achievable thrust for a given specific impulse. This can be seen from the Child-Langmuir equation and from the expression for the thrust in GIEs.

The Child-Langmuir equation yields the maximum current density. The ion beam current density J_i (A/m^2) for singly ionized ions with $V_{12} \gg kT_e$, is derived from the Child-Langmuir law and can be written as:

$$J_i = \frac{4\varepsilon_0}{9}\sqrt{\frac{2e}{m_i}}\frac{V_{12}^{3/2}}{d^2} \tag{1}$$

where J_i is the current density of ions (A/m^2), ε_0 is the permittivity of vacuum, e is the electron charge, m_i is the ion mass, V_{12} is the electric potential difference between the screen grid (grid 1) and the acceleration grid (grid 2) and d is the distance between grid 1 and grid 2.

Assuming that the beam is comprised of singly ionized ions and diverges uniformly and has a constant ion current density profile that is accelerated by a uniform electric field [2], the expression for the thrust of a GIE is:

$$T = \sqrt{\frac{2m_i}{e}}J_i A_g T_g cos\theta \sqrt{V_t} \tag{2}$$

where T is the thrust produced by the ions (in Newtons), A_g is the grid area, T_g is the transparency of the grid (%), θ is the half angle of divergence of the beam and V_t is the total potential drop of the ion beam current between the discharge chamber and the last grid. For a neutralised beam, $V_t = V_{12}$ for GIE2 and $V_t = V_{13}$ for GIE3.

In order to increase the thrust it is necessary to increase the ion current $(I_i = J_i A_g T_g)$ or the voltage V_t $(V_t = V_{12}$ in GIE2 and $V_t = V_{13}$ in GIE3) or the area A_B - or a combination of these parameters. However, in GIE2-3, for a given distance between the grids, d, there is a maximum voltage V_{12} before arcing between the grids occur and excessive curvature of the plasma sheath in the discharge chamber cause the ions to impact grid 1. Therefore, increasing the voltage V_{12} will require an increase in the distance, d, between grids 1 and 2, reducing the current density. This

---

compromise limits the maximum ion beam current achievable with GIE2-3s. Increasing the area A_B to achieve higher thrust levels can be unpractical due to limitations in launcher's payload volume and launch costs. The possible maximum practical diameter for a GIE is around 40 cm, as used in the NASA's NEXT thruster [3]. Therefore, there is a need for increasing the thrust density – thrust per unit of area - of the GIE without increasing its volume.

2. The Dual-Stage Four Grid Ion Engine (DS4G)

To address the need for higher thrust density a novel GIE concept was envisioned by D. Fern [4]. In this concept the ion extraction – and therefore the current density – and the ion acceleration processes are decoupled. This is achieved with the addition of an extra grid with relation to the GIE3 or two grids with relation to the GIE2. Figure 1 shows the DS4G thruster concept. The screen grid (grid 1) has the same function as in the GIE2-3. The second grid is the extraction grid, but differently from the GIE2-3 it does not also has the function of accelerating the ions to high velocities. Instead, the second grid in the DS4G is responsible for maximizing the ion beam current and is at much lower potentials than in a traditional GIE2-3 making it possible for the screen grid and extraction grid (grids 1 and 2) distance to be much smaller than in the GIE2-3. Nevertheless, the extraction grid also gives the ions an initial velocity. The third grid is the acceleration grid, where very high potentials can be applied up to at least 80 kV [5] with relation to the extraction grid. This will enable the DS4G to achieve specific impulses as high as 30000s while keeping the ion beam current density constant, therefore making it possible to increase the thrust density (N/m^2).
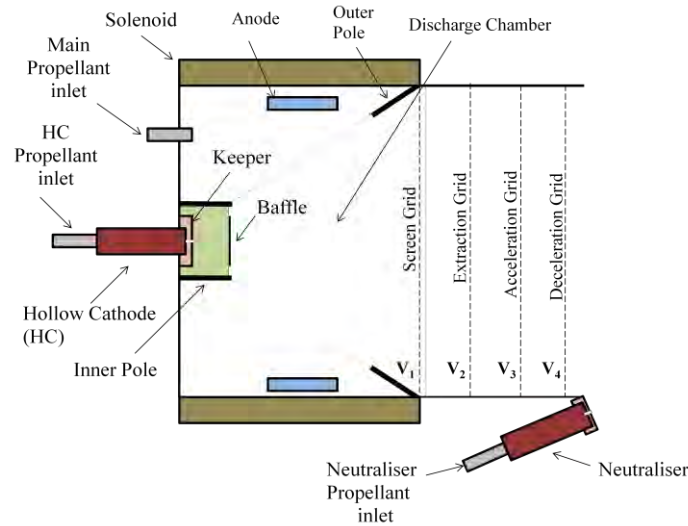
Figure 1: Dual-Stage Four Grid (DS4G) ion thruster

3. Performance equations

In the analysis of the performance of gridded ion engines (GIEs), DS4G and GIE2-3, it is important to define some performance equations. The beam power P_b (W) is given by:

$$P_b = I_i V_t \tag{3}$$

The electrical efficiency η_e is given by [2]:

$$\eta_e = \frac{P_b}{P_{in}} \tag{4}$$

where P_{in} is the total input power given to the thruster.

The total input power, P_{in}, is the sum of the ion beam power and all the power required to generate the ion beam and will include the electrical power of the cathode heater and keeper or RF generator, grids and losses. The total power input to the thruster, P_{in} can be written as:

$$P_{in} = P_b + P_d + P_c + P_n + P_{g1} + P_{g2} + P_{g3} + P_{g4} + P_s + P_L$$

where P_d is the power in the main discharge, P_c is the power in the hollow cathode-keeper (or the RF generator), P_n is the power in the neutralizer, P_{g1} to P_{g4} are the power in the grids 1-4 due to ion beam impingement and ion

backstreaming from the plume (P_{g4}), P_s is the power of electromagnets that provide the magnetic field in the discharge chamber and P_L is due to other power losses.

The propellant utilisation efficiency η_m is given by:

$$\eta_p = \frac{\dot{m}_i}{\dot{m}} = \frac{I_i}{e}\frac{m_i}{\dot{m}} \tag{5}$$

where $\dot{m}$ is the total propellant mass flow rate (kg/s).

The total efficiency η_T can be then defined as:

$$\eta_T = \frac{P_{jet}}{P_{in}} = cos\theta \, \eta_p \eta_e = cos\theta \, \frac{\dot{m}_i}{\dot{m}}\frac{P_b}{P_{in}} \tag{6}$$

where P_{jet} is the total power in the exhaust jet.

Because $P_{jet} = \frac{1}{2}\dot{m}V_{ex}^2 \cos\theta$ and $T = \dot{m}V_{ex}$ we can write that $P_{jet} = \frac{T^2}{2\dot{m}}\cos\theta$ and that:

$$\eta_T = \frac{T^2}{2\dot{m}\,P_{in}}\cos(\theta) = \frac{cos\theta}{2\dot{m}P_{in}}\left[\frac{4\varepsilon_0}{9}\frac{\sqrt{m_i}V_{ex}^{1.5}A_gT_gI_{sp}g_0}{\eta_p\sqrt{e}\,d^2}\right]^2 \tag{7}$$

But also because:

$$P_{jet} = P_i + P_N = \left(\frac{1}{2}\dot{m}V_e^2\right)\eta_p + \left(\frac{1}{2}\dot{m}V_{e0}^2\right)(1-\eta_p) \tag{8}$$

where P_i is the power of the ionized ejected mass, P_N is the power of the non-ionized (neutrals) ejected mass, V_e is the velocity of the ionized mass, V_{e0} is the velocity of the neutrals mass, we can then write:

$$P_{jet} = \frac{1}{2}\dot{m}_iV_e^2 + \frac{1}{2}\dot{m}_0V_{e0}^2 \tag{9}$$

where $\dot{m}_i$ is the ion mass flow rate, $\dot{m}_0$ is the neutrals mass flow rate.

The specific impulse can be defined as:

$$I_{sp} = \frac{cos\theta \, \eta_p}{g_0}\sqrt{2V_t\frac{e}{m_i}} \tag{10}$$

4. Scaling of GIEs

For a given beam divergence, θ, propellant efficiency, η_p, and propellant ion mass, m_i, for singly ionised ions, the specific impulse I_{sp} of the GIEs depends on the total potential that the ion current is subjected, V_t. Fig. 2 shows plots of the I_{sp} for general cases of the GIE2-3 ($\theta_{GIE} = 15°$, $\eta_p = 90\%$) and DS4G ($\theta_{GIE} = 4°$, $\eta_p = 90\%$), for the propellants Argon (Ar) and Xenon (Xe).
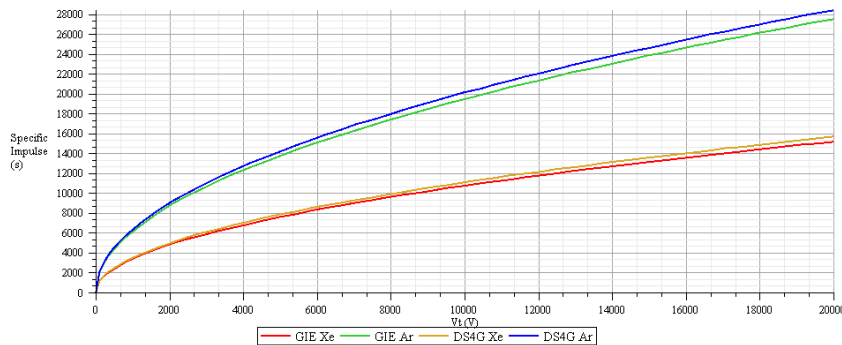
Fig. 2: Specific Impulse for the GIE2-3 and DS4G as a function of the plasma potential V1 (0 to 20kV).

The current density increases as the distance between grids 1 and 2 are reduced. However, the distance between grid 1 and grid 2 is limited by the maximum electric field before arcing occurs and also to avoid excessive curvature of the plasma sheath which could cause the ions to impinge on the extraction (DS4G)/acceleration (GIE2-3) grid. In this work

the maximum electric field of 1kV/mm will be used. Figure shows the minimum distance between grids 1 and 2, d_{12}, for a given potential difference between the grids, V_{12}, and its correspondent maximum ion current density, J_i , for singly ionised ions, assuming a maximum electric field of 1kV/mm and that $V_{12} \gg kT_e$.
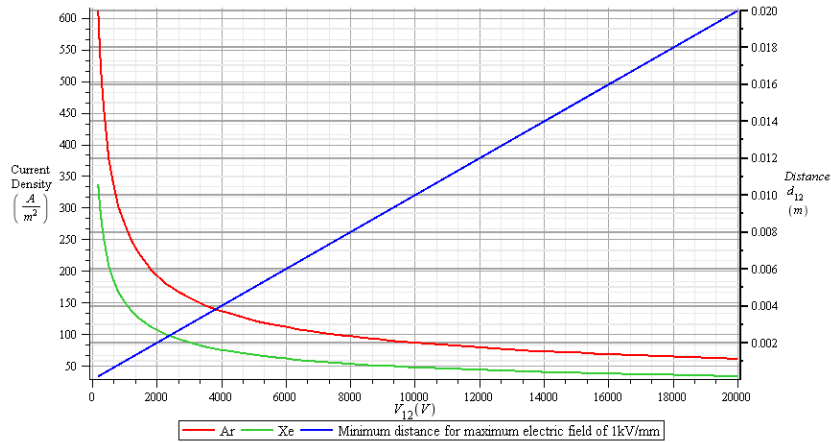
Figure 3: Maximum ion current density (J) and minimum distance between grids 1 and 2 (d_{12}) as a function of the electric potential difference V_{12} (200V to 20kV).

The ideal ion current, I_i, is selected differently for the GIE2-3 and for the DS4G, as in the GIE2-3 there is a compromise between the ion current and the thrust produced and in the DS4G this is decoupled. Figure shows the ion current for five different diameters of the extraction grid (40, 50 and 60 cm).
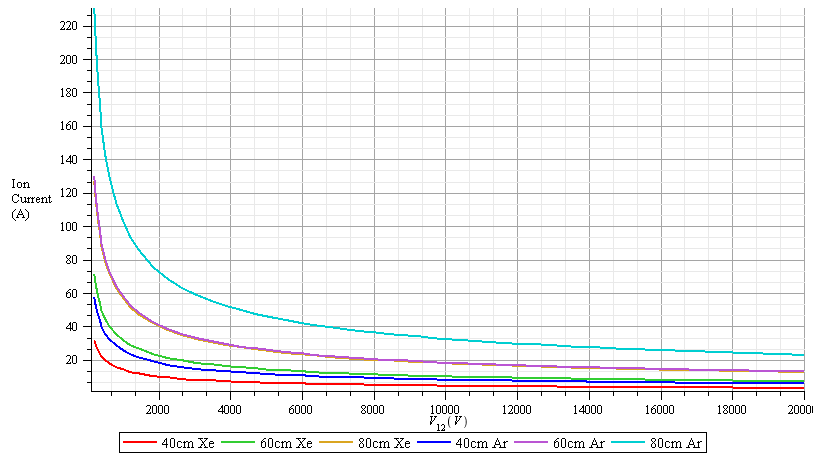
Figure 4: Ion Current for 5 extraction grid diameters with transparency at 60% as a function of V_{12} (200V to 20kV).

The thrust in the GIE2-3 is limited by the maximum electric field that can be applied between the screen grid (grid 1) and the extraction and acceleration grid (grid 2) and also by the grid area, A_g, and the divergence angle, θ. The maximum electric field that can be applied between grids 1 and 2 depends on several parameters, such as the ion current, the efficiency of the discharge chamber, grid surface roughness, amongst other factors. In this work, the value of 1kV/mm was used. Therefore, if the electric field is maintained constant and at the maximum value of 1kV/mm – and therefore the distance d_{12} changing accordingly - for a certain grid area, A_g, the thrust is practically constant for the range 1kV-80kV.

In the DS4G the extraction potential and the acceleration potential are independent and it is possible to have a higher thrust for the same grid diameter, compared to the GIE2-3. Figure shows the GIE3 thrust for 3 different grid diameters with a transparency $T_g = 75\%$, $\theta = 15^o$, $V_{12} = 0.95\,V_t$ and also shows the DS4G thrust for three different grid diameters with $T_g = 75\%$ and $\theta = 4^o$, $V_{12} = 1000V$.
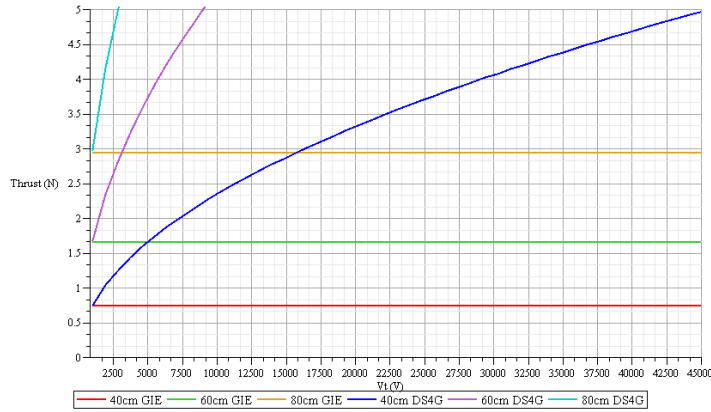
Figure 5: GIE2-3 Thrust for three different diameters of grid and $T_g = 75\%$, $\theta = 15^o, V_3 = -50V$ and DS4G thrust for three different diameters of grid and $T_g = 75\%$, $\theta = 4^o, V_{12} = 1000V$

With a maximum electric field of 1kV/mm applied between grids 1 and 2 in both the GIE3 and DS4G, the thrust density of the DS4G can be much higher than the GIE2-3. Figure shows the thrust density for the GIE3 and for the DS4G.
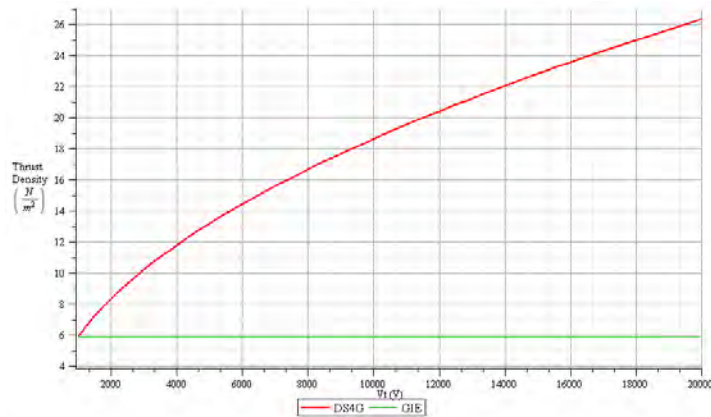
Figure 6: DS4G ($\theta = 4^o$) and GIE2-3 ($\theta = 15^o$) thrust density for $T_g = 75\%$ and electric field at 1kV/mm.

It is also useful to compare the thrust density as a function of the specific impulse for both the GIE2-3 and the DS4G, as shown in Figure
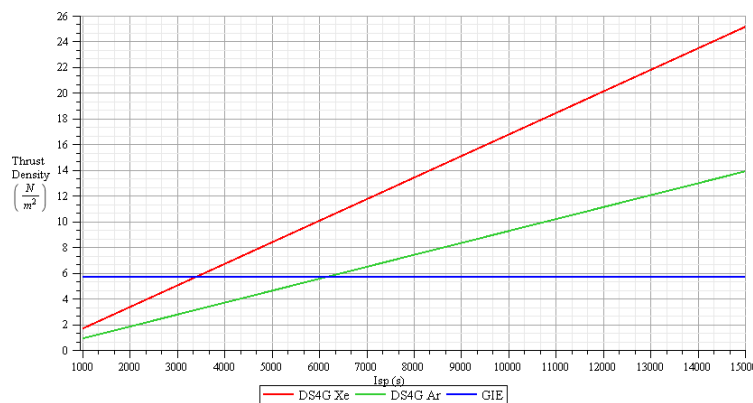
Figure 7: Thrust density as a function of the specific impulse for the GIE2-3 and the DS4G.

The total efficiency, η_T, of the GIE2-3 and the DS4G depends on the electric efficiency, η_e, propellant utilisation efficiency, η_p, and beam divergence, θ. The total efficiency is highly dependent on the implementation of the discharge chamber and ion optics. To understand the trend of the efficiency of GIEs it is convenient to write the expression of the total efficiency as:

$$\eta_T = \frac{P_{jet}}{P_{in}} = \frac{P_{jet}}{P_o + P_{jet}} = \frac{1}{1 + \frac{P_o}{P_{jet}}} \tag{11}$$

where P_o is all the power that is not in the exhaust jet, i.e., $P_o = P_d + P_c + P_n + P_{g1} + P_{g2} + P_{g3} + P_{g4} + P_s + P_L$ and is the "cost" to produce the ions. Assuming that P_o is constant, we can see the trend of the total efficiency as calculated analytically and shown in Figure 2.
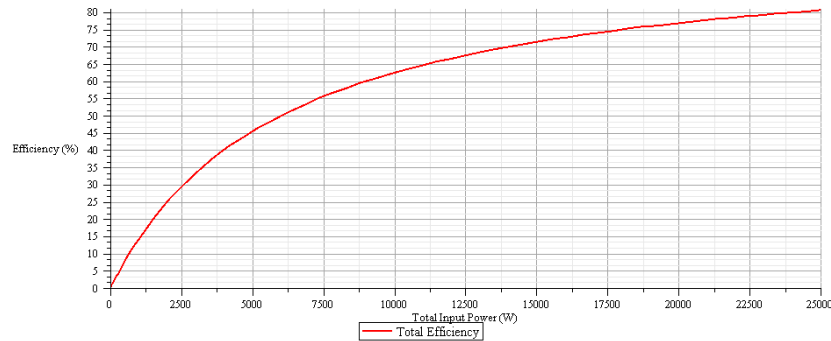
Figure 2: Trend of the total efficiency in GIEs (GIE2-3 and DS4G) calculated analytically.

5. Preliminary DS4G thruster design for high Delta-V missions

Two levels of power were envisioned to be used in clusters of a specific number of thrusters in different missions. Following the HiPER project guidelines, thrusters of 25kW and 50kW were considered. This was done to avoid having too many separate thruster designs - leading to the use of one design for each specific mission case and redundancy scheme - with the aim of having fewer thruster designs each of which can meet more than one set of mission requirements. As this design exercise is considered to be zeroth order, the variations in thruster performance with changes in thrust and specific impulse have not been included. The same assumptions made earlier in this paper are valid here, i.e., $T_g = 75\%$, $\theta_{DS4G} = 4^o$. The thrusters selected are DS4G ion engines using Xenon fuel.
Table 1 shows a detailed view of the results.

Table 1: Preliminary Design of the DS4G Ion Thrusters for each mission class.

Mission Class	Thruster Power Class (kW)	Specific Impulse (s)	Thrust (N)	Total Accelerating Potential (V)	Thrust Density (N/m²)	Thruster Grid Area (m²)	Thruster Grid diameter (m)	Thruster Length (m)	Thruster Total Diameter (m)	Ion Beam Current (A)	Total Ion Beam Power (kW)	Total Input Power (kW)	Power to thrust ratio (kW/N)
Infra-structure to Earth-Moon L1	25	5000	0.82	2030	8.40	0.10	0.35	0.48	0.48	11.03	22.39	**25.26**	30.81
		10000	0.45	8120	16.77	0.03	0.18	0.25	0.25	3.03	24.62	**25.41**	56.47
Mars Sample Return	25	5000	0.82	2030	8.40	0.10	0.35	0.48	0.48	11.03	22.39	**25.26**	30.81
		10000	0.45	8120	16.77	0.03	0.18	0.25	0.25	3.03	24.62	**25.41**	56.47
NEO NEP	25	5500	0.76	2450	9.22	0.08	0.32	0.44	0.44	9.31	22.82	**25.24**	33.21
	50	5500	1.51	2450	9.22	0.16	0.46	0.62	0.62	18.51	45.34	**50.15**	33.21
NEO SEP	25	6100	0.69	3020	10.23	0.07	0.29	0.40	0.40	7.62	23.02	**25.00**	36.23
	50	6100	1.38	3020	10.23	0.13	0.41	0.57	0.57	15.24	46.04	**50.00**	36.23
NEP Missions to Jupiter	25	5000	0.82	2030	8.40	0.10	0.35	0.48	0.48	11.03	22.39	**25.26**	30.81
		10000	0.45	8120	16.77	0.03	0.18	0.25	0.25	3.03	24.62	**25.41**	56.47
		15000	0.31	18260	25.16	0.01	0.13	0.17	0.17	1.39	25.42	**25.79**	83.18
	50	5000	1.63	2030	8.40	0.19	0.50	0.68	0.68	21.93	44.51	**50.21**	30.81
		10000	0.89	8120	16.77	0.05	0.26	0.35	0.35	6.00	48.70	**50.26**	56.47
		15000	0.61	18260	25.16	0.02	0.18	0.24	0.24	2.74	50.03	**50.74**	83.18
NEP missions to Saturn	25	5000	0.82	2030	8.40	0.10	0.35	0.48	0.48	11.03	22.39	**25.26**	30.81
		10000	0.45	8120	16.77	0.03	0.18	0.25	0.25	3.03	24.62	**25.41**	56.47
		15000	0.31	18260	25.16	0.01	0.13	0.17	0.17	1.39	25.42	**25.79**	83.18
	50	5000	1.63	2030	8.40	0.19	0.50	0.68	0.68	21.93	44.51	**50.21**	30.81
		10000	0.89	8120	16.77	0.05	0.26	0.35	0.35	6.00	48.70	**50.26**	56.47
		15000	0.61	18260	25.16	0.02	0.18	0.24	0.24	2.74	50.03	**50.74**	83.18
Mars Infra-structure	25	8000	0.55	5190	13.42	0.04	0.23	0.31	0.31	4.63	24.04	**25.24**	45.89
	50	8000	1.09	5190	13.42	0.08	0.32	0.44	0.44	9.18	47.63	**50.02**	45.89

6. References

[1]   Dan M. Goebel and Ira Katz, "Fundamentals of Electric Propulsion: Ion and Hall Thrusters", NASA Jet Propulsion Laboratory, California Institute of Technology, March 2008.

[2]   Wilbur, P. J., "Limits on High Specific Impulse Ion Thruster Operation", *AIAA Proceedings of the Joint Propulsion Conference*, AIAA paper, 2004-4106, Fort Lauderdale, 2004.

[3]   D. Herman, "Discharge Cathode Electron Energy Distribution Functions in   a   40-cm   NEXT-type   Ion Engine," AIAA-2005-4252, 41st AIAA Joint Propulsion Conference, Tucson, Arizona, July 10–13, 2005.

[4]   Fearn, D G, "The use of ion thrusters for orbit raising", *Journal of the British Interplanetary Society*, Vol. 33, pp. 129-137, 1980.

[5]   C. Bramanti, D. G. Fearn, "The Design and Operation of Beam Diagnostics for the Dual Stage 4-Grid Ion Thruster", 30th International Electric Propulsion Conference, Florence - Italy, September 17-20, 2007.